

# Porous anodized aluminium oxide: application outlooks

N. Tsyntsaru<sup>1,2</sup>

<sup>1</sup> Institute of Applied Physics of ASM,  
Chisinau, MD-2028,  
Academiei 5, Moldova

<sup>2</sup> Faculty of Chemistry,  
Vilnius University,  
LT-03325 Vilnius,  
Naugarduko St. 24, Lithuania

Properties of nanomaterials often differ from the ones of macrosized materials, and many of them have to be investigated. As one of the example is the formation of porous anodic metal oxides. An oxide film can be grown up on certain metals by anodization, the so-called valve metals. For each of these metals there are conditions established to enable promotion of the formation of thin, dense, barrier or porous oxide having uniform thickness at the whole surface. Among valve metals aluminum is an important case because of its ability to find diverse and important applications including architectural finishes, prevention of corrosion of automotive and aerospace structures, and electrical insulation. The porous aluminium anodic oxide (AAO) collected an enormous attention, because its pores can be used as a template for preparing various nanomaterials as nanoparticles, nanowires and nanotubes. The most widely used baths contain sulfuric acid, for particular applications oxalic or phosphoric acids are also used. It has been widely accepted mechanism that the formation of pores in anodized metal oxides is based on two continuous processes, one is oxide dissolution at the electrolyte/oxide interface and the other is oxidation of metal at the oxide/metal interface. This work presents an overview on fabrication research, understanding the formation mechanism of anodic metal oxide and the application of different sized AAO materials.

**Keywords:** anodic aluminium oxide, macro- and nanosized oxide, sulfuric, oxalic and phosphoric acids, mechanical and tribological properties, electrodeposition, wettability

## INTRODUCTION

Aluminum, when is anodized, forms self-organized arrays of cylindrical pores, and this phenomenon was detected by Keller et al. [1]. In 1995, a highly ordered anodic aluminum oxide (AAO) with self-organized hexagonal arrays was reported by Masuda and Fukuda [2], and later on the AAO template was widely used to produce nanowires of various metals [3–5]. The pore size and interval between pores in anodized aluminum oxide (AAO) can be tuned between ca 2 nm and 1 micron depending on the anodization conditions [6]. Due to this ample range of the pore size, AAO membranes are used as templates in a variety of nanotechnology applications without the need for expensive lithographical techniques [7].

The formation of porous alumina depends upon the current density or voltage employed for anodizing, and the temperature, pH and composition of the electrolyte. These parameters determine the extent of chemical interaction between the anodic alumina and the electrolyte during anodizing. Such

interaction is accelerated by the electric field [8]. After anodization, the films comprise a barrier layer next to the metal and an outer barrier layer, in which the pores are orientated normal to the film surface [1]. The topography of the AAO film as well as the formation rate of the oxide layer depends on the anodization condition which is closed related to the types of electrolyte, concentration, temperature and applied voltage.

To date, the most popular model explaining the self-adjustment of pores in AAO is based on the mechanical stress associated with expansion of aluminum during the oxide formation. This is the cause of a repulsive force between neighboring pores, which leads to the self-ordering process [7]. Mainly, the following chemical processes dominate the anodization of the alumina membranes [9, 10].

(1)  $\text{Al}^{3+}$  ions form at the metal/oxide interface and distribute in the oxide layer near the oxide/metal interface:



(2) The electrolysis of water occurs at the pore bottom near the electrolyte/oxide interface:

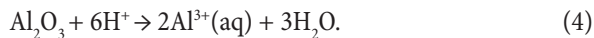
\* Corresponding author. E-mail: ashra\_nt@yahoo.com



(3) Due to the electric field, the  $\text{O}^{2-}$  ions migrate within the barrier layer from the electrolyte/oxide interface to the oxide/metal interface, and react with the  $\text{Al}^{3+}$  ions there, forming  $\text{Al}_2\text{O}_3$ :



(4) And there is an electric-field-enhanced oxide dissolution at the electrolyte/oxide interface:



In the anodization process of the porous alumina membranes, there is a balance between the electric-field-enhanced oxide dissolution at the electrolyte/oxide interface and the formation of oxide at the oxide/metal interface. This balance is crucial to the formation of the porous alumina membranes, since it makes the thickness of the barrier layer constant in the entire anodization process and hence allows steady-state pore propagation into the Al.

## EXPERIMENTAL

Experiments were carried out according to the scheme given in Fig. 1. In order to obtain well-ordered porous AAO with various pore diameters anodisation in different baths, namely, sulphuric, oxalic and phosphoric acids, was carried out. After production of the samples, characterization of mechanical, tribological and wetting properties were performed, including possibilities to electrodeposit Co nanowires.

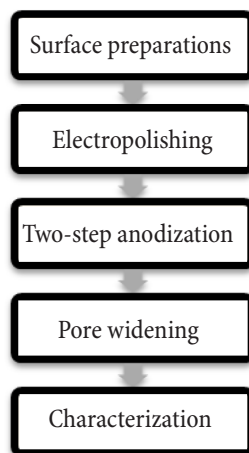


Fig. 1. Experiment flow chart

The most important step in the pre-treatment of aluminum before anodizing is the polishing of the samples. For aluminum, this can be achieved by means of mechanical, chemical, or electrochemical polishing; in our case, electrochemical polishing in a 60%  $\text{HClO}_4 + \text{C}_2\text{H}_5\text{OH}$  (1:4, v/v) solu-

tion at 10 °C and 500 mA/cm<sup>2</sup> for 1 min was used to prepare smooth Al surfaces before anodizing.

During the 1st anodization, the pore structure on the surface is badly arranged. By removing this non-regular oxide layer, a periodic concave pattern is formed on the aluminum surface. Then the 2nd anodization was carried out at the same anodizing potential as that used for the 1st anodization, thus, forming well-ordered AAO surfaces. The anodization was carried out in sulfuric, oxalic or phosphoric acids at voltages of 19–25, 40–60 and 160–195 V, respectively.

Conventionally, AAO is fabricated under the so-called “mild anodization” (MA), where a low voltage is applied. However, MA results in pore sizes in the range of only several tens of nanometer to maximum around 100 nm. Thus, in order to obtain larger pore sizes the so-called “hard anodization” (HA), which was introduced in the 1960s [11], was employed. The basic concept of HA takes advantage of the high voltage ( $\geq 120$  V) so that anodization progresses at a very high speed. Meanwhile, the temperature of the electrolyte is kept at a low value (typically below 2 °C) with a magnetic bar stirring to avoid local heating.

**Post-etching.** The post-etching step is also called the pore opening step, which mainly uses a chemical etching to broaden the pores. Phosphoric acid is the most widely used solution in post-etching and 5% is the preferred concentration.

## RESULTS AND DISCUSSION

### Porous film growth

It is generally accepted that the porous structure of the anodic alumina film develops from the barrier-type coating formed on aluminum at the start of anodization. Growth of the barrier film occurs due to the high field ionic conduction and the constant field strength, defined as a ratio of the potential drop across the barrier film to its thickness [12]. Governed by the constant field strength, the uniform film with a uniform current distribution is developed on the whole surface. The uniform growth results in a smoothing effect on the initial roughness of the aluminum. However, some local variations in field strength can appear on a surface with defects, impurities or preexisting features including sub grain boundaries, ridges and troughs as remains of pre-treatment procedures [11]. This non-uniform current distribution leads consequently to the enhanced field-assisted dissolution of oxide and a local thickening of the film. The higher current above metal ridges, accompanied by a local Joule heating, results in the development of a thicker oxide layer [13]. Recently, the local heat transfer on current density was studied for anodizing in sulfuric acid [14]. It was found that increasing the local temperature enhances the local field assisted oxide dissolution at the pore base, and consequently increases the local current density. According to [11] the oxide layer grown above the ridges is prone to generate a highly localized stress. Consequently, successive cracking of the film and its rapid healing occurs at the high local current density. Therefore, with a consumption of aluminum base

and enhanced progress in the oxide thickness build-up above the flaw sites, the crack-heal events are more pronounced and the curvature of the film increases at the oxide/metal interface. Shimizu et al. [15] suggested that a tensile stress at surface ridges leads to the formation of cracks which can act as conductive pathways for film growth and where a rapid healing effect occurs. The preferential growth of oxide above flaw sites, and thickening of the barrier layer, proceed continuously until the moment when the current is concentrated in the thinner film region at the bottom of the future pore. On the other hand, increasing pore curvature (increasing pore diameter) decreases the effective current density across the barrier layer. As a result, the growth of other pores from other incipient pores is initiated in order to maintain a uniform field strength across the barrier layer. When the curvature of the oxide film at the oxide/metal interface has increased sufficiently and intersection of the scalloped regions has occurred, the steady-state conditions of pore growth are reached. For steady state porous oxide growth, there is a dynamic equilibrium between oxide growth at the oxide/metal interface and field-assisted oxide dissolution at the electrolyte/oxide interface.

Before anodizing, a surface pre-treatment is essential for obtaining the best self-organized porous structures. The main aim of this pre-treatment is to reduce the faults on the surface as much as possible (Fig. 2).

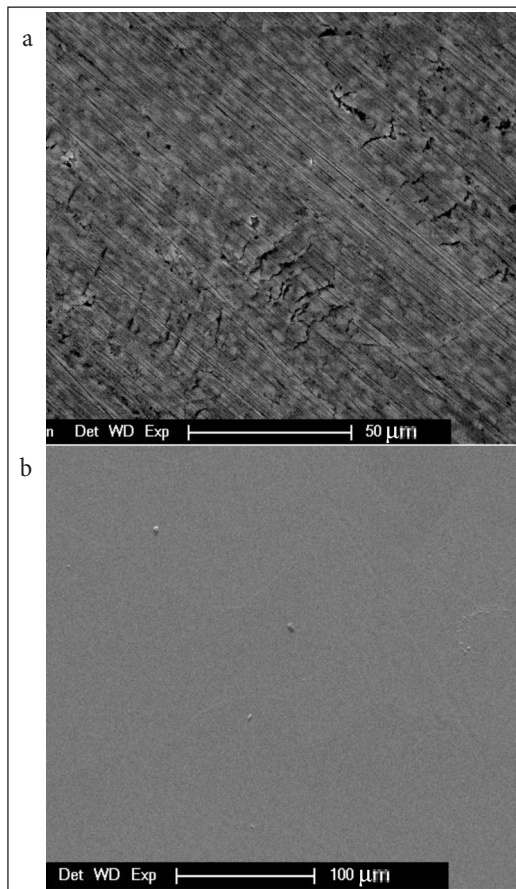


**Fig. 2.** SEM image of the Al surface: prior to electropolishing (a); after electropolishing (b)

The regularity of the pores and pore arrangement commonly increases with the anodization time, especially during the first several hours. Therefore, a conventional one-step anodization process with a relatively long anodization period will result in alumina membranes with disordered pores on the top and regular pores at the bottom of the membranes (Fig. 3a).

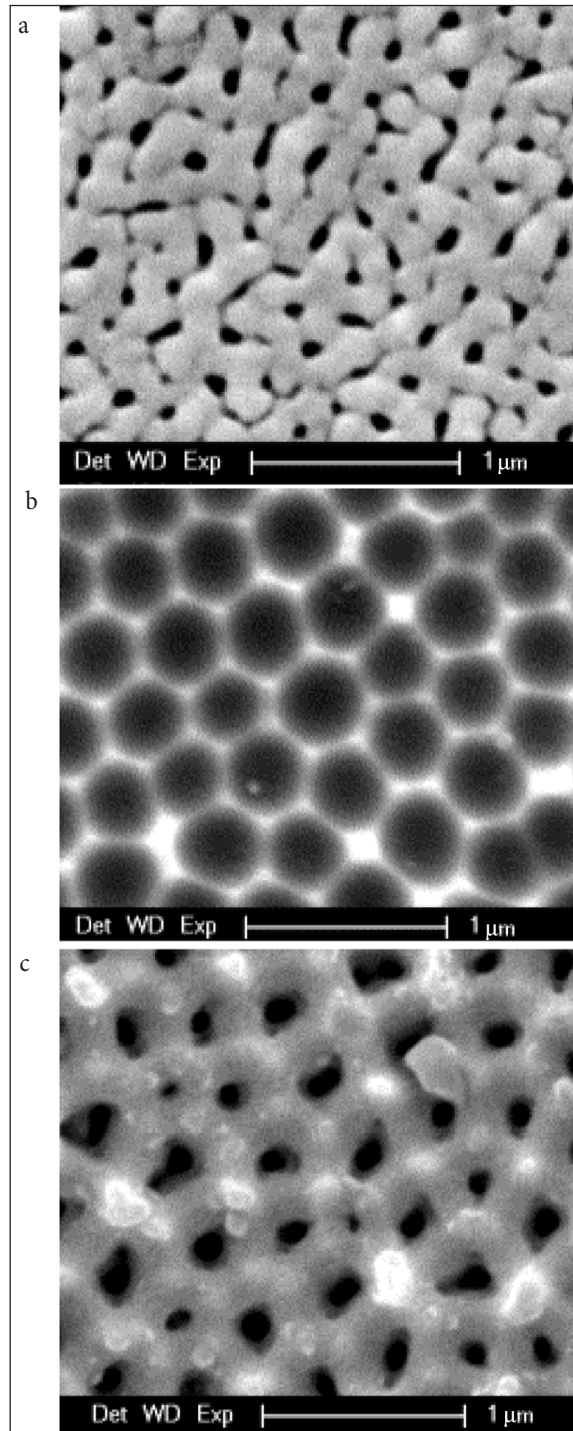


**Fig. 3.** Cross section SEM images for samples prepared in 5% phosphoric acid: after 1st anodization (a), after oxide removal (b), after 2nd anodization (c)

A two-step anodization process that was proposed by Masuda and Fukuda [2] successfully realized the fabrication of alumina membranes with regular pores throughout the entire membranes. Since then, this method has become the standard way for the preparation of highly ordered AAO structures. In this process, after a long first anodization, the top-distorted first alumina layer is removed from the Al foil, leaving a highly ordered concave pattern on the surface of the Al foil (Fig. 3b). Then, a second anodization is carried out on this surface-patterned Al foil, resulting in alumina membranes with regular pore arrays at both sides of the membranes (Fig. 3c).

Anodization in three studied acids resulted in well-ordered porous AAO materials (Fig. 4). Thus, depending on the electrolyte used and voltage applied different size pores can be obtained.

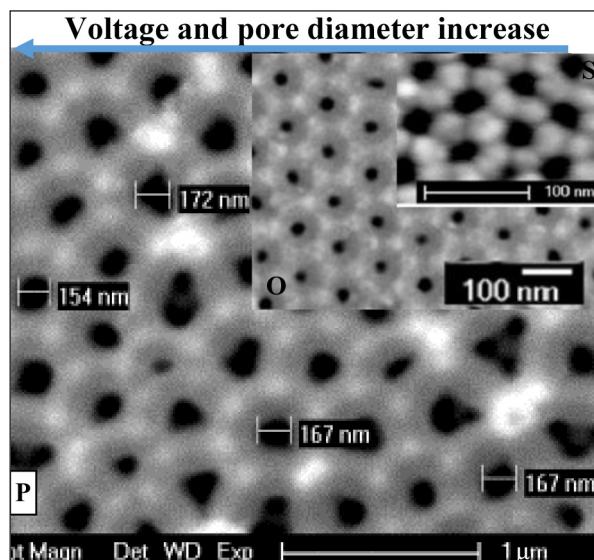


**Fig. 4.** SEM images of hexagonally distributed well-ordered nanoporous AAO produced: in sulphuric acid (S) at potential of 21 V; in oxalic acid (O) at potential of 70 V; in phosphoric acid (P) at potential of 175 V

## CHARACTERIZATION OF POROUS AAO FILMS

### Mechanical and tribological behaviour of AAO

After the discovery of nano-porous materials, the definition of nanoporous materials seems to be confusing. The IUPAC categorized nanoporous materials in three categories: microporous, mesoporous and macroporous materials [16]. The definition of them is as follows: microporous materials mean those nanoporous materials with pore diameters less than 2 nm, mesoporous materials are materials containing nanopores with diameters between 2 and 50 nm, and macroporous materials are those nanoporous materials having pore widths greater than 50 nm.

In this part of the paper we will focus on mechanical and tribological properties of mesoporous AAO, namely produced from sulphuric and oxalic acids. Nanoindentation tests were

performed over a wide range of normal loads (5 to 100 mN) to study the mechanical behaviour of anodized aluminium oxides. Loading rates were as twice as the peak load applied per minute (e. g.  $10 \text{ mN}\cdot\text{min}^{-1}$  for 5 mN max load). Indentation imprints were observed by SEM. Loading vs penetration depth data were recorded. Hardness values were measured by the Oliver & Pharr method. Representative SEM images of the imprints are given in Fig. 5. Since AAO is a ceramic material, crack formation and propagation was expected as a result of nanoindentation. But SEM images revealed an interesting response. The oxide layer was only deformed locally, where the indenter was in contact with the surface. AAO did not respond by formation of any major cracks either inside or outside the imprint which was a different result from Ng et al. reported in [17]. The so-called bilinear cracks were not observed on samples neither produced in sulphuric acid nor in oxalic acid [18].

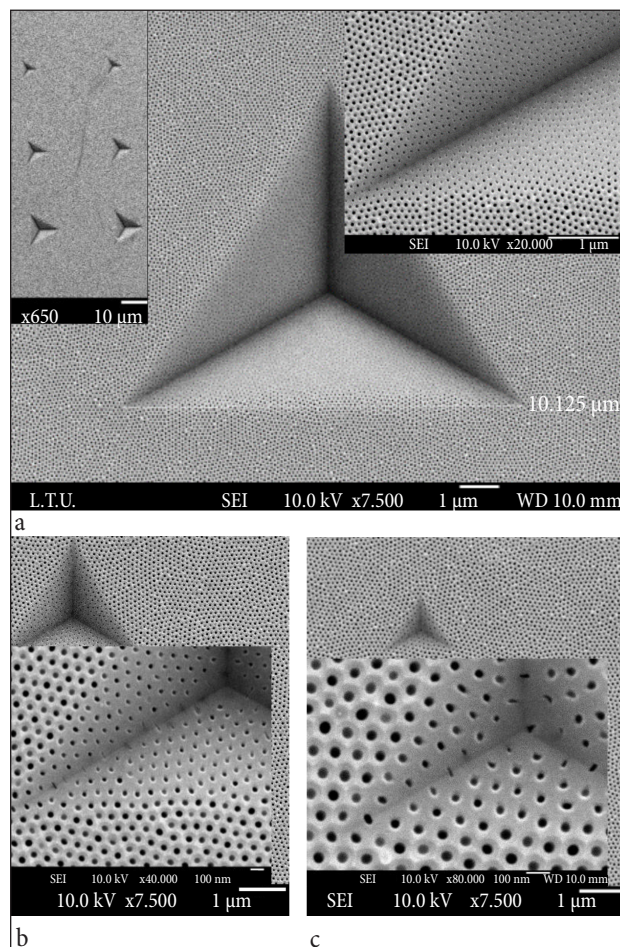


**Fig. 5.** SEM images of nanoindentation imprints under different loads on mesoporous AAO: 100 mN (a), 50 mN (b), 20 mN (c)

Tribological characterization was performed in order to evaluate how AAO would behave under biaxial loading. Ball-on-flat tests were run to apply bidirectional loading. The wear mechanism was investigated in relation to the pore diameter, porosity percentage and oxide composition. To avoid possible tribochemical reactions, a ball

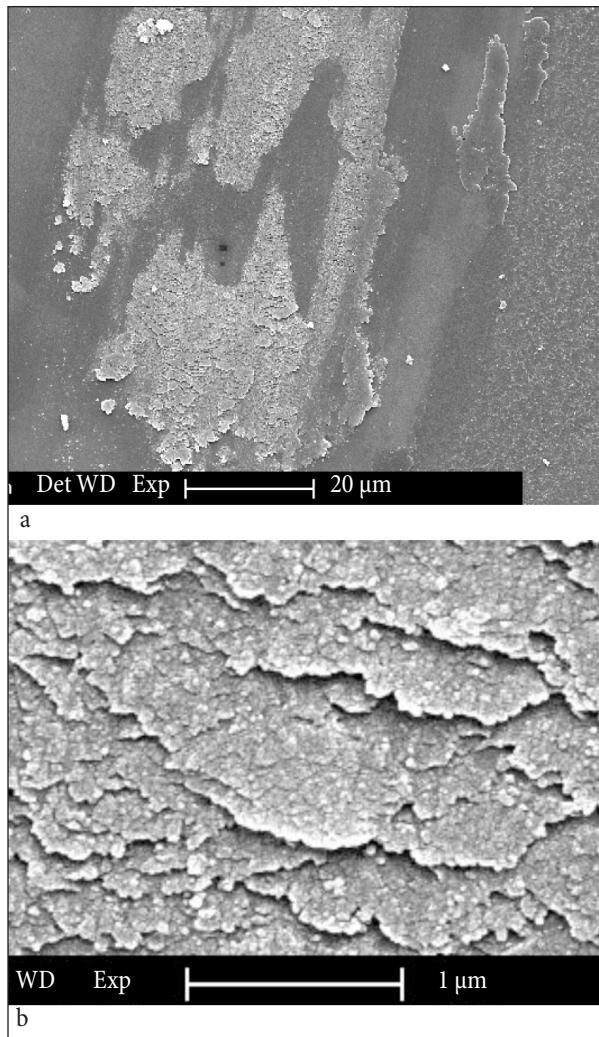


**Fig. 6.** SEM images of the wear tracks on AAO produced from sulfuric acid after 1000 cycles and under 1000 mN normal load; an overall view (a) and the edge of the wear track at high magnification (b)

counterbody made of corundum with a 5 mm diameter was employed.

Wear tracks were examined using SEM (Fig. 6a). At high magnifications an interesting response was realized (Fig. 6b). Pores were started to be filled in by fine debris particles without any cracking. This behaviour proved that the tubes were strong enough to resist bidirectional loading. After 1000 cycles, surface was covered by thick debris with the same appearance independent from the load applied. This shows that abrasive wear in the beginning caused formation of wear particles as the third body which made the relative motion harder due to an adherent behaviour. Thus, the wear mechanism was a combination of abrasive and adhesive wear resulting in a high coefficient of friction, but without essential damages of AAO.

**The application of AAO as template materials**

The macroporous confined method is a method which grows one-dimensional (1D) nanomaterials into specific diameter nanopores. Therefore the diameter of the forming one-dimen-

sional nanomaterials will be confined to the same diameter of nanopores or below the diameter of nanopores. Among many different methods, such as vacuum evaporation [19], magnetron sputtering [20], electroless deposition [21] and electroplating [22], the last one seems to be a simple, efficient and cheap approach for the fabrication of metallic nanowires into templates. Advantages of electrodeposition include a strict control of the nanowire length, chemical composition of nanowires (fabrication of alloy nanowires), and the achievement of different segments with different compositions along the nanowire length (fabrication of multilayered nanowires) [23].

We tried to fabricate the cobalt nanowires into AAO templates using the alternating current (AC) method. Following the second anodization in sulphuric acid, the voltage was systematically reduced to promote thinning of the barrier layer, then Co nanowires were electrodeposited. The AC electrodeposition was carried out using a 200 Hz sine waveform (reductive time = oxidative time = 2.5 ms) in which the deposition voltage was 30 V<sub>p-p</sub>. Cobalt filled up the entire pores, and it is deposited on the bulk too. But the SEM images after FIB milling (Fig. 7, inset) revealed pictures different from the SEM images of the alumina cross-section (Fig. 7). Although cobalt was deposited along the entire length of the AAO template, the true picture (inset) of the alumina template filled by cobalt nanowires suggests to us that Co nanowires can be deposited by this method, but only short ones, due to hydrogen evolution and peculiarities of diffusion in pores, which will affect the uniformity of filling.

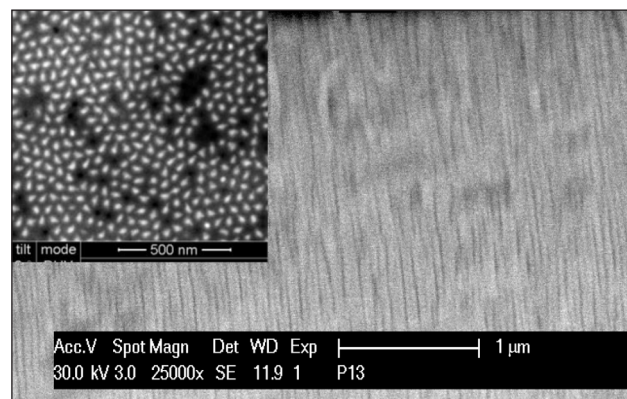


**Fig. 7.** SEM images of the AAO cross-section filled by Co nanowires and the top surface of the ion-milled Co-filled template at a depth of 6 μm from the top of 12 μm deep-pores (inset)

**Wetting properties of macroporous AAO**

The wettability studies on AAOs started only in recent years, most of the work being focused on fabricating super hydrophobic AAOs by surface modification. A controlled topography can be fabricated and further investigation of the wettability dependence on the topography which has been studied is needed. The challenge is to find out whether AAOs with stable

as well as desired wettability can be obtained. This will supply valuable information for industrial applications as well. Another perspective is foreseen for the rapidly growing field of nanotechnology, since more and more scientists working in this domain are using AAOs to grow nanowires by electrodeposition, an intensive understanding of the wettability of AAOs might be helpful in order to obtain nanowires with the desired and well-controlled pore characteristics. The wettability of the hydrophobic AAO films is similar to the “rose petal effect”, where water droplets stick to the surface even when turned upside down. For the AAO fabricated in phosphoric acid, the oxide layer thickness is found to have little influence on the wettability within a critical thickness range. For a larger film thickness, the wetting contact angle (WCA) decreases significantly. This critical value is closely related to the pore size. Values were found to be around 3.0 and 4.2  $\mu\text{m}$  for pore sizes within the range of 150–200 and 370–420 nm, respectively. The WCA is found to increase with the pore size within the range of 200–420 nm. For even larger pore sizes, the WCA decreases first slightly, then dramatically due to the destruction of the AAO structure. The highest WCA achieved on pure AAO is 127.5° (Fig. 8); this value corresponds with a pore size in the range of 370–420 nm. On the other hand, the WCA on the pure untreated, and non-porous, aluminum substrate is found to be around 80 [24]. Combining both desired topography and surface chemistry, the highest WCA measured on modified AAO samples can be 135.6° (Fig. 8, inset).

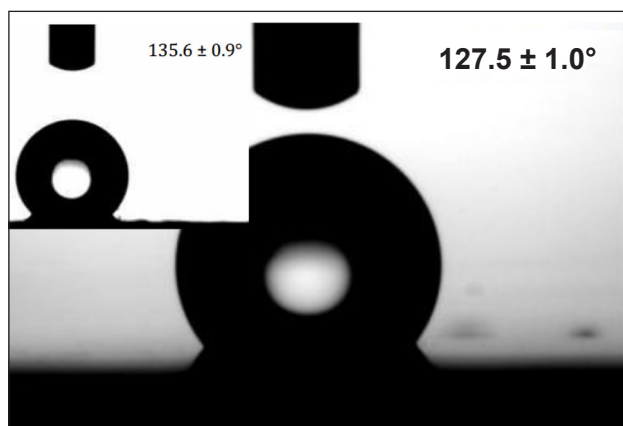


**Fig. 8.** The wetting contact angle measured on AAO produced from phosphoric acid and on AAO modified with lauric acid (inset)

## CONCLUSIONS

The macroporous and mesoporous anodic aluminium oxides obtained from sulphuric, oxalic and phosphoric acids have been investigated in details. Mechanical properties and frictional behaviour of AAO were investigated depending on the porosity percentage and the anodization bath used. Normal loading by nanoindentation did not reveal any major crack propagation on AAO. The penetration depth was

highly affected by the porosity percentage. Although no major cracks were observed, minor cracks were present on samples with sulphur contamination. Wear caused formation of a thick, compacted and sparsely distributed debris with a highly adherent behaviour. Pores were partially filled with debris in the beginning of the fretting test.

Also, the possibility has been demonstrated to deposit Co under AC electrodeposition in the produced mesoporous AAO. Different electrochemical conditions were applied for the template synthesis of cobalt nanowire arrays. The study under different AC conditions such as current frequencies (50–1000 Hz) and  $V_{p-p} = 30$  V revealed that the optimal frequency is in a range of 150–200 Hz.

The important difference between mesoporous and macroporous AAO has been shown on the example of wettability study. For this purpose layers with pore sizes in a range of 150–200 nm was fabricated by hard anodization in phosphoric acid. Combining appropriate topography and chemistry (lauric acid), the WCA of AAO samples produced from phosphoric acid can be modified from 127 to 135.6°.

## ACKNOWLEDGEMENTS

The authors acknowledge funding from HORIZON2020 SELECTA Project (642642) and FP7 Oil & Sugar Project (295202). Also, partial funding was granted by the Research Council of Lithuania (MIP-031/2014) and Moldavian national projects (15.817.02.05A), (14.819.02.16F).

Received 23 November 2015

Accepted 1 December 2015

## References

1. F. Keller, M. S. Hunter, D. L. Robinson, *J. Electrochem. Soc.*, **100(9)**, 411 (1953).
2. H. Masuda, K. Fukuda, *Science*, **268(5216)**, 1466 (1995).
3. D. G. W. Goad, M. Moskovits, *J. Appl. Phys.*, **49(5)**, 2929 (1978).
4. A. Jagminiene, G. Valincius, A. Riaukaite, A. Jagminas, *J. Cryst. Growth*, **274(3–4)**, 622 (2005).
5. A. Yamaguchi, F. Uejo, T. Yoda, et al., *Nat. Mater.*, **3(5)**, 337 (2004).
6. S. Z. Chu, K. Wada, S. Inoue, M. Isogai, Y. Katsuta, A. Yasumori, *J. Electrochem. Soc.*, **2006(9)**, B384 (2006).
7. O. Jessensky, F. Müller, U. Gösele, *J. Appl. Phys.*, **72**, 1173 (1998).
8. S. J. Garcia-Vergarai, L. Iglesias-Rubianesi, C. E. Blanco-Pinzon, P. Skeldon, G. E. Thompson, P. Campestrini, *Proc. Roy. Soc. Lond. A*, **462(2072)**, 2345 (2006).
9. F. Li, L. Zhang, R. M. Metzger, *Chem. Mater.*, **10**, 2470 (1998).
10. G. E. Thompson, G. C. Wood, in: J. C. Scully (ed.), *Treatise on Materials Science and Technology*, Vol. 23, Ch. 5, pp. 205–329, Academic Press Inc., New York (1983).

11. W. Lee, R. Ji, U. Gosele, K. Nielsch, *Nat. Mater.*, **5**(9), 741 (2006).
12. G. E. Thompson, *Thin Solid Films*, **297**, 192 (1997).
13. J. P. O'Sullivan, G. C. Wood, *Proc. Roy. Soc. Lond. A*, **317**(1531), 511 (1970).
14. I. De Graeve, H. Terryn, G. E. Thompson, *J. Appl. Electrochem.*, **32**(1), 73 (2002).
15. K. Shimizu, K. Kobayashi, G. E. Thompson, G. C. Wood, *Phil. Mag. A*, **66**(4), 643 (1992).
16. J. Rouquerol, D. Avnir, C. W. Fairbridge, et al., *Pure Appl. Chem.*, **66**, 1739, 1745 (1994).
17. K. Y. Ng, Y. Lin, A. H. W. Ngan, *Acta Mater.*, **57**, 2710 (2009).
18. N. Tsyntaru, B. Kavas, J. Sort, M. Urgan, J.-P. Celis, *Mater. Chem. Phys.*, **148**(3), 887 (2014).
19. K. Yasui, K. Nishio, H. Masuda, *Jpn. J. Appl. Phys.*, **44**(37-41), L1181 (2005).
20. L. S. Zhang, P. X. Zhang, Y. Fang, *Anal. Chim. Acta*, **591**(2), 214 (2007).
21. A. Azizi, M. Mohammadi, S. K. Sadrnezhad, *Mater. Letters*, **65**(2), 289 (2011).
22. N. J. Gerein, J. A. Haber, *J. Phys. Chem. B*, **109**(37), 17372 (2005).
23. G. D. Sulka, L. Zaraska, W. J. Stepniowski, in: *Encyclopedia of Nanoscience and Nanotechnology*, 2nd edn., Vol. 11, pp. 261–349, American Scientific Publishers (2011).
24. J. G. Buijnsters, R. Zhong, N. Tsyntaru, J.-P. Celis, *ACS Appl. Mater. Interfaces*, **5**(8), 3224 (2013).

N. Tsyntaru

#### **PORĖTAS ANODIZUOTAS ALIUMINIO OKSIDAS: PRITAIKYMO APŽVALGA**

##### *S a n t r a u k a*

Straipsnyje pateikta trumpa porėtojo aliuminio oksido gavimo sieros, oksalo ir fosforo rūgštyse ypatumų, savybių, formavimosi mechanizmo bei taikymo galimybių apžvalga. Mechaninės savybės, trinties koeficientas aptariami juos siejant su porėtumo dalimi paviršiuje ir anodavimo tirpalo sudėtimi. Taip pat aptariamos galimybės elektrochemiškai nusodinti kobaltą aliuminio oksido mezoporose. Svarbūs makro ir mezoporėto aliuminio oksido skirtumai parodyti tiriant vilgymo kampus.